Proceedings Paper:

Hoang, K.D. orcid.org/0000-0001-7463-9681, Atallah, K., Birchall, J. et al. (1 more author) (2019) Comparative evaluation of simplified and complex IPM machine models on control development for traction applications. In: Proceedings of IECON 2019 - 45th Annual Conference of the IEEE Industrial Electronics Society. IECON 2019 : 45th Annual Conference of the IEEE Industrial Electronics Society (IES), 14-17 Oct 2019, Lisbon, Portugal. IEEE , pp. 945-950. ISBN 9781728148793

https://doi.org/10.1109/IECON.2019.8926742

Comparative Evaluation of Simplified and Complex IPM Machine Models on Control Development for Traction Applications

Khoa Dang Hoang and Kais Atallah
Dept. of Electronic and Electrical Engineering
The University of Sheffield
Sheffield, United Kingdom
https://orcid.org/0000-0001-7463-9681
https://orcid.org/0000-0002-8008-8457

Jeff Birchall and Stuart Calverley
Magnomatics Limited
Park House, Bernard Road
Sheffield, S2 5BG, United Kingdom
j.birchall@magnomatics.com
s.calverley@magnomatics.com

***Abstract*—The paper presents a comparative evaluation of simplified and complex interior permanent magnet (IPM) machine models for control development in traction applications. It is shown that although control implementation using the complex model could result in better IPM machine performances, in practice, validation of complex model is significantly complicated and deviations from assumed parameters may compromise the performance of the control scheme. It is demonstrated that the simplified model of which validation is simpler may provide similar performance compared with the complex model. Thus, the simplified model-based control method can be considered for traction applications at the earlier stage of control development or when validation of the complex machine model is difficult.**

Keywords—Control development, maximum torque per ampere (MTPA) control, IPM machine, traction applications.

I. INTRODUCTION

Due to its rotor structure resulting in its high efficiency and depth of field weakening (FW) operation ability [1], interior permanent magnet (IPM) machine is often employed under torque control mode within its full torque-speed range for traction application [2], Fig. 1(a). Since IPM machines are well-known for their nonlinear characteristics [3]-[4], control methodology using predefined look-up tables (LUTs) of *dq*-axis current references with inputs as torque and speed (or flux) demands are often employed for high performance targets, Fig. 1(b), [5]. Therefore, accurate information of the tested IPM machine model including nonlinear parameters as a function of full range of *dq*-axis currents considering both saturation and cross-coupling effects [5] are highly desired for development of *dq*-axis current reference LUTs. In practice, validations of IPM machine parameters [6]-[7] often involves injection of different *dq*-axis current sets into the machine, collect relevant data (voltages, currents, torque), and post-measurement processing. Obviously, this validation process is complicated and measurement errors resulting in mismatch issue are inevitable. Therefore, at the earlier stage of control development of traction application, a simple and reliable machine model with acceptable accuracy for consideration as an initial control model is essential. It is noted that for IPM machine, saturation effect is mainly contributed by the *q*-axis current whereas cross-coupling effect is caused by both *dq*-axis current components. Also, IPM machine with single layer rotor is often employed for traction application due to its robust mechanical structure [2], [8] and this rotor geometry is the main focus of the paper.

The paper presents a comparative evaluation of simplified IPM machine model considering only saturation effects and complex IPM machine model accounting for both saturation and cross-coupling effects on control development for traction applications. It is shown that the simplified IPM machine model of which validation is simpler may provide machine performances similar to the complex model. Thus, control development using the simplified model can be considered for control development of traction applications at the earlier stage or when validation for the complex machine model is difficult.

The paper content is as follows. Mathematical models for IPM traction machine and its performance are discussed in the section II. Complex and simple models of the tested IPM machine together with development of its relevant *dq*-axis LUT current references are introduced in the section III. Section IV compares and discusses the tested IPM machine performances using the simplified *dq*-axis LUT current references and complex *dq*-axis LUT current references. Some conclusions are presented in the section V.

II. IPM MACHINE MODEL AND OPERATION REGIONS

A. IPM Machine Model for Control Development

According to [3]-[5], the mathematical model in *dq*-axis reference for IPM machine is as follows.

$$v_d = R_s i_d - \omega_e \psi_q \;;\; v_q = R_s i_q + \omega_e \psi_d \tag{1}$$

$$\psi_d = L_d i_d + \psi_m \;;\; \psi_q = L_q i_q \tag{2}$$

$$T_e = (3/2)p[\psi_m + (L_d - L_q)i_d]i_q \tag{3}$$

where $v_{d,q}$, $i_{d,q}$, $\psi_{d,q}$, $L_{d,q}$ are the transformed (*dq*) voltages, currents, stator flux-linkages, and stator inductances, respectively; ω_e is the stator electrical frequency; R_s is the stator resistance; T_e is the machine torque; ψ_m is the PM flux linkage.

Under space vector modulation (SVM) and considering over-modulation implementation [3], maximum achievable phase voltage V_{max} is expressed in (4) where V_{dc} is the *DC*-link voltage; k_{mi} is the modulation index constant which depends on the selected over-modulation technique.

$$V_m = \sqrt{v_d^2 + v_q^2} \le V_{\max} \;;\; V_{\max} = k_{mi} V_{dc} \tag{4}$$

In addition, the machine current is limited by a maximum value I_{max} associated with the selected cooling method and winding insulation class.

$$\sqrt{i_d^2 + i_q^2} \le I_{\max} \tag{5}$$

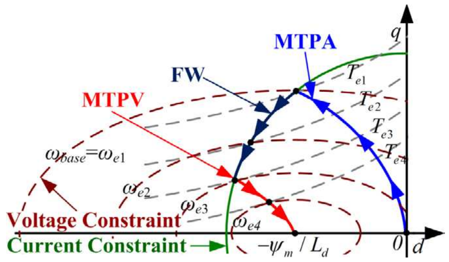

(a)

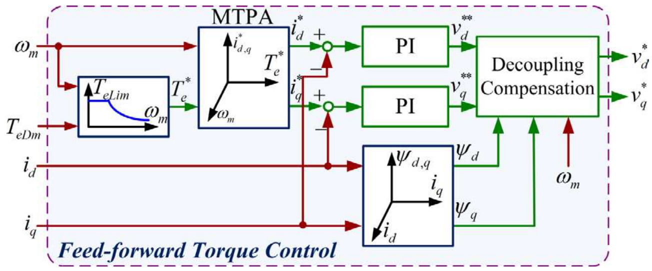

(b)

Fig. 1. Control of IPM machine. (a) Operation regions. (b) Control strategy.

B. IPM Machine Operation Regions

Operation regions for IPM machine is illustrated in Fig. 1(a) [1]. As can be seen, in the low-speed operation region when the machine voltage is still lower than the maximum achievable voltage V_{max}, the maximum torque per ampere (MTPA) operation can be employed [3]-[4]. For a demanded torque, relevant *dq*-axis current references can be determined by solving (6) and then (3). Therefore, the following equation is satisfied:

$$(L_d - L_q)^2 i_q^4 + \frac{2T_e}{3p}\psi_m i_q - \left(\frac{2T_e}{3p}\right)^2 = 0 \tag{6}$$

In the high-speed operation region, under a demanded torque, *dq*-axis current references are selected to maintain both demanded torque and voltage limit as shown in the FW region in Fig. 1(a), and (7) is satisfied. It is noted that stator resistance voltage drop is neglected in (7). It is also noted that the maximum achievable current I_{max} is still achievable in the FW operation region. However, in deep FW operation, for a given maximum achievable voltage (4), there is a maximum achievable torque associated with this maximum voltage (or its relevant flux) (8). This operation region limited by this maximum achievable torque is named as maximum torque per voltage (MTPV). As can be seen, maximum achievable current is not maintained in this operating mode, Fig. 1(a).

$$a_4 i_d^4 + a_3 i_d^3 + a_2 i_d^2 + a_1 i_d + a_0 = 0 \tag{7}$$

where

$$a_0 = -\psi_m^2 B + \left(\frac{2T_e}{3p}L_q\right)^2; a_1 = 2L_d\psi_m^3 - 2AB\psi_m$$

$$a_2 = L_d^2\psi_m^2 + 4L_d\psi_m^2 A - BA^2; a_3 = 2L_d\psi_m A^2 + 2A\psi_m L_d^2$$

$$a_4 = L_d^2 A^2; A = L_d - L_q; B = \psi_{\max}^2 - \psi_m^2$$

$$\psi_{\max} = V_{\max} / \omega_e = \sqrt{\psi_d^2 + \psi_q^2}$$

$$2(L_d - L_q)\psi_d^2 + L_q\psi_m\psi_d - (L_d - L_q)\psi_{\max}^2 = 0 \tag{8}$$

It is noted that the *dq*-axis inductances and the PM flux linkage values in (1) to (3) and (6) to (8) are nonlinear and often described as a function of *dq*-axis currents [3]-[5].

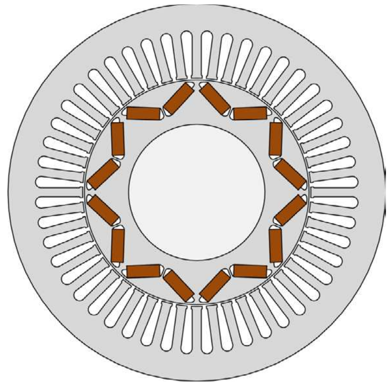

(a)

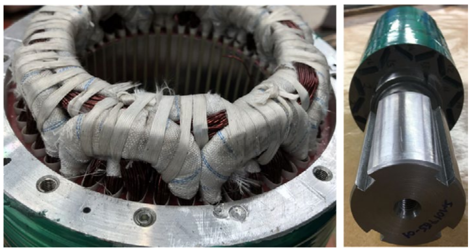

(b)

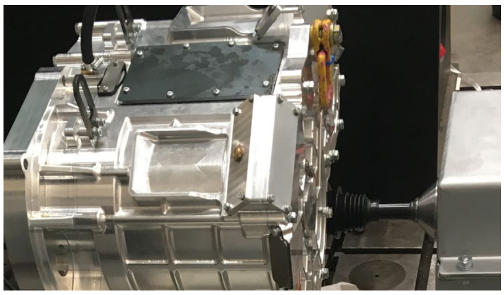

(c)

Fig. 2. Studied IPM traction machine. (a) Geometries. (b) Prototype. (c) Hybrid powertrain integrating IPM machine.

TABLE I

SPECIFICATIONS OF TESTED IPM MACHINE

Peak torque (Nm)	225
Continuous torque (Nm)	112.5
Peak current (A)	340
Base speed (rpm)	4850
Maximum speed (rpm)	14500
DC-link voltage (V)	600
Number of pole pair	4

III. MODEL-BASED CONTROL DEVELOPMENT FOR IPM MACHINE

Control development for IPM considering nonlinear machine parameters were presented in [3]-[5]. Although online control method may offer more control flexibilities [3], [4]; offline control strategy using predefined *dq*-axis current reference LUTs is often employed for traction application due to its simpler implementation [5]. Fig. 1(b) illustrates an example of offline control method where predefined *dq*-axis current reference LUTs of which inputs are demanded torque and instantaneous operating speed. It is noted that these *dq*-axis current reference LUTs cover full aforementioned torque-speed operation regions of the IPM traction machine under control. Generation of these LUTs will be discussed in the next section.

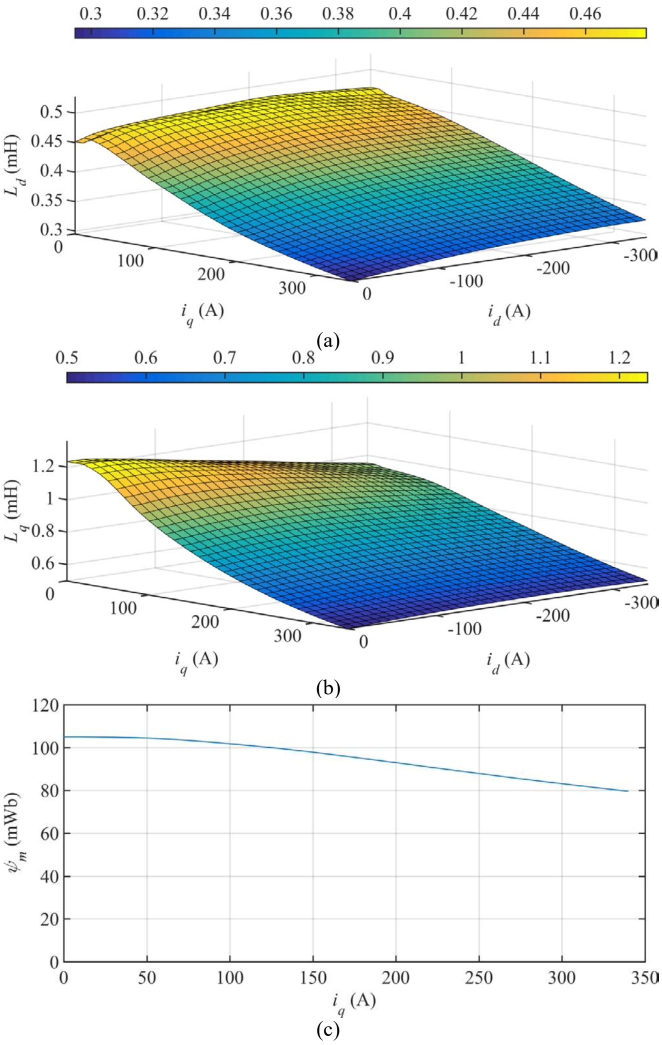

Fig. 3. Complex model of tested IPM machine parameters. (a) *d*-axis inductance. (b) *q*-axis inductance. (c) PM flux linkage.

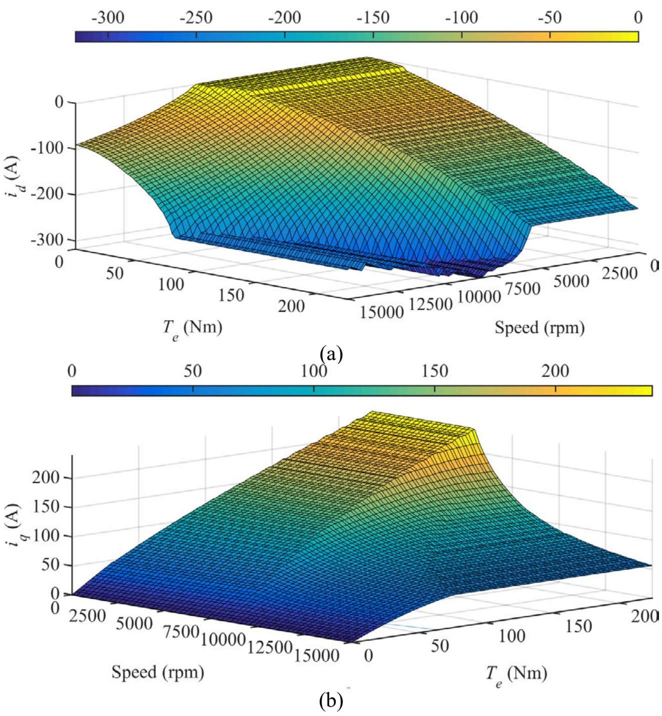

Fig. 4. Complex model-based *dq*-axis current reference LUTs. (a) *d*-axis current reference. (b) *q*-axis current reference.

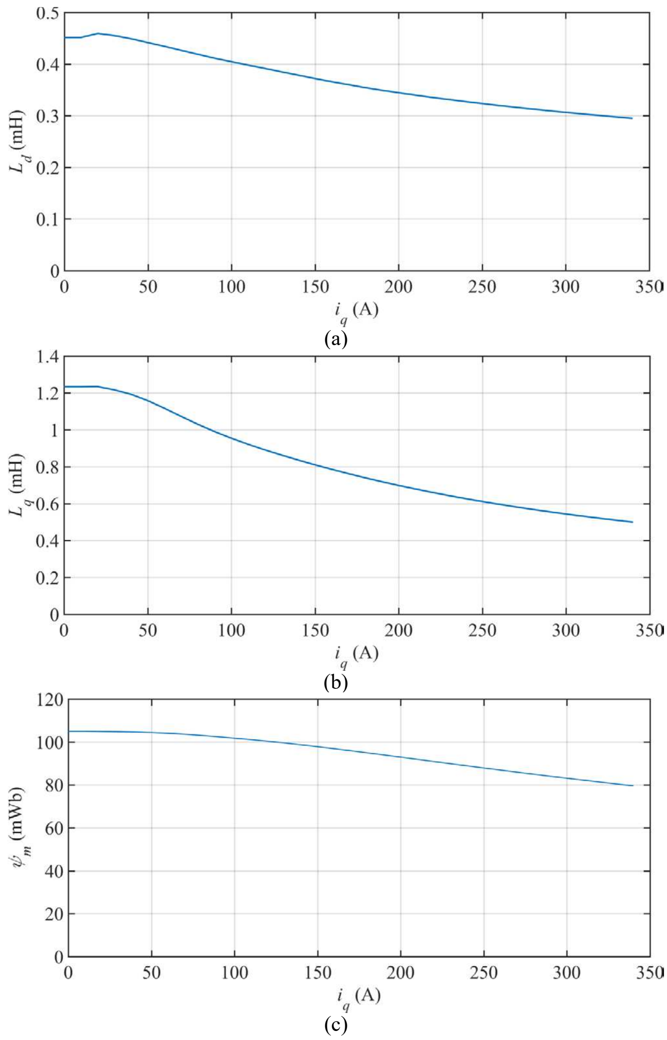

Fig. 5. Simplified model of tested IPM machine parameters. (a) *d*-axis inductance. (b) *q*-axis inductance. (c) PM flux linkage.

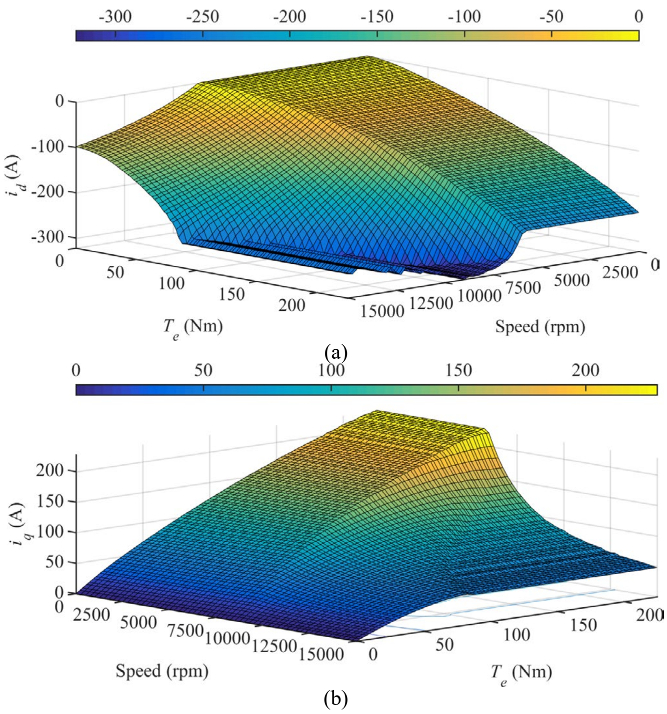

Fig. 6. Simplified model-based *dq*-axis current reference LUTs. (a) *d*-axis current reference. (b) *q*-axis current reference.

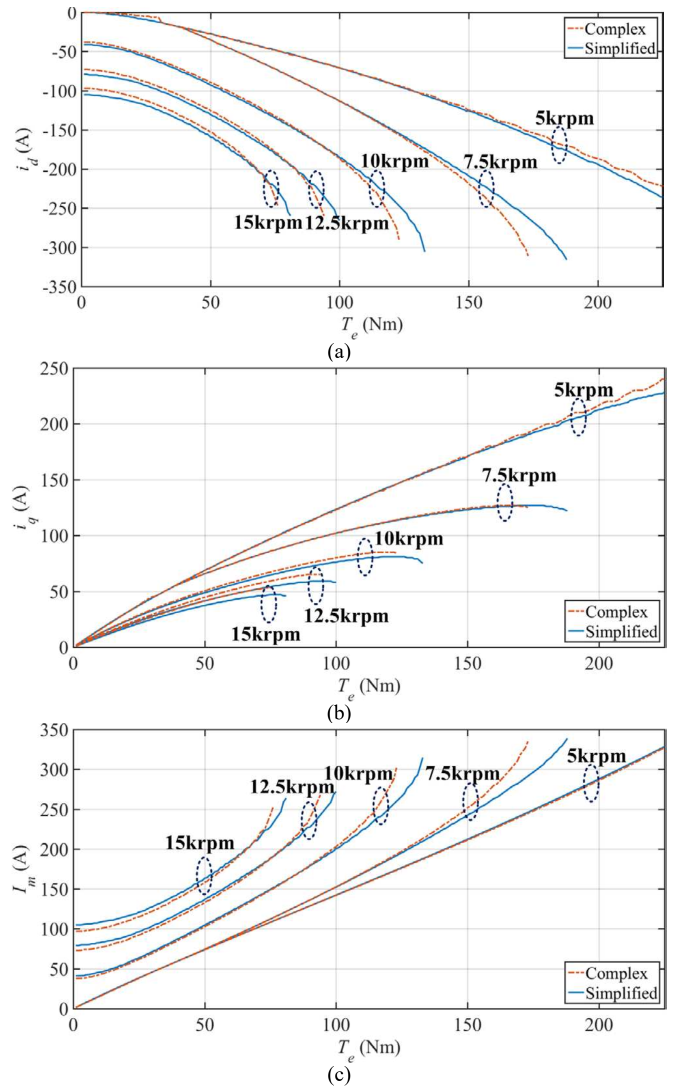

Fig. 7. Comparative study between complex and simplified machine model. (a) *d*-axis current reference. (b) *q*-axis current reference. (c) Current magnitude.

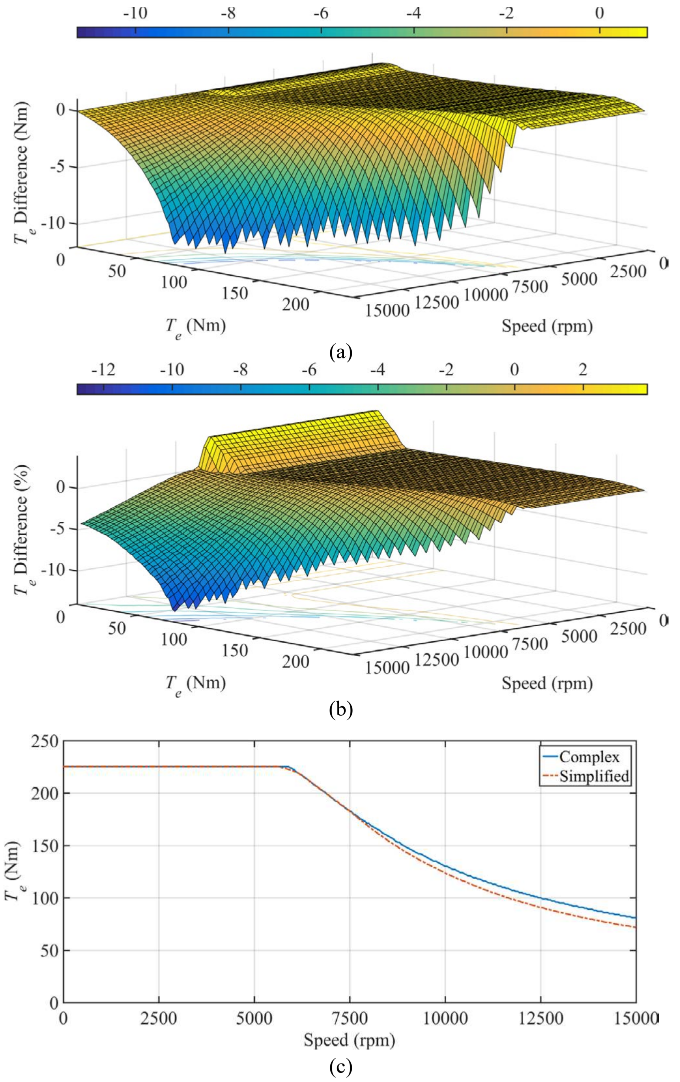

Fig. 8. Difference in torque between complex and simplified machine models. Torque in Nm. (b) Torque in percentage. (c) Torque-speed envelope.

A. Complex Model-based Control Development

The control methodology in Fig. 1(b) was employed for an IPM traction machine developed for integrating into a hybrid powertrain and schematics/prototype and parameters/specifications are depicted in Fig. 2 and Table I, respectively. The tested IPM machine is equipped with single layer rotor which is often employed for traction application due to its robust mechanical structure [2]. First, the machine nonlinear parameters were generated from FEA or validated via measurement [6], [7], Fig. 3. Then, for a given torque-speed operation point, variation of *dq*-axis currents from zero to their maximum values considering maximum achievable voltage and current is implemented to find proper sets of *dq*-axis currents satisfying the demanded torque. Finally, the optimum *dq*-axis current references are selected for achieving the demanded torque with minimum current, Fig. 4. As can be seen, this control development method can satisfy MTPA control by obtaining demanded torque with minimum required current magnitude; FW operation by considering both current and voltage boundary; and MTPV operation by considering voltage boundary. However, this method depends on machine parameters which essentially requires measurement validation. In practice, validation of IPM machine parameters often requires injection of different sets of *dq*-axis currents into the machine, collect relevant data (voltages, currents, torque), and post-measurement processing to obtain *dq*-axis inductance and PM flux linkage, Fig. 3. Obviously, this validation process is complicated and measurement errors and temperature variations may compromise the machine performance.

B. Simple Model-based Control Development

The machine nonlinear characteristic shown in Fig. 3 is affected by saturation mainly caused by *q*-axis current and cross-coupling effect [6], [7]. As can be seen in Fig. 3, for the tested IPM traction machine, the nonlinear characteristic is predominantly affected by *q*-axis current. Fig. 5 presents the simple nonlinear machine model considering only effect of *q*-axis current. It is noted that the PM flux linkage is the same for both the two models. Based on this model, *dq*-axis current reference LUTs are generated and depicted in Fig. 6.

IV. Comparative Study Between Complex Model-based and Simple Model-based Current Reference LUTs

Current references under different demanded torque and operation speed using complex-based model, Fig. 4, and simplified-based model, Fig. 6, are illustrated in Fig. 7. As

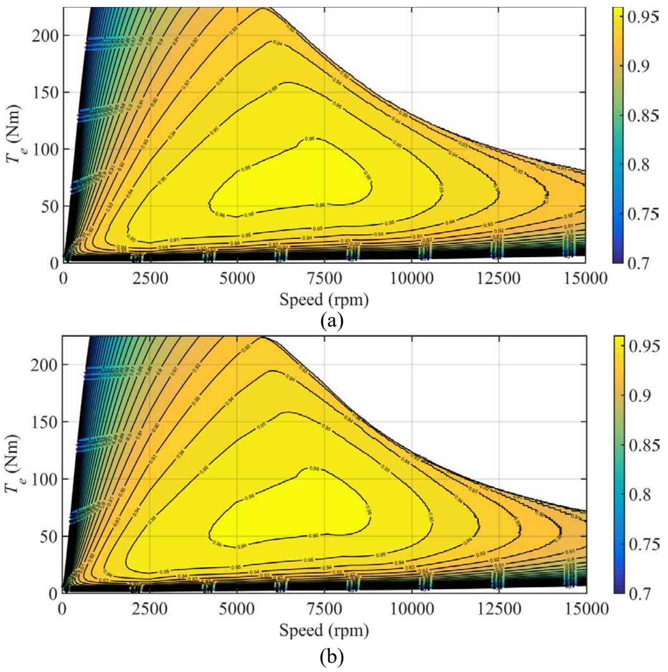

Fig. 9. Tested IPM traction machine efficiency. (a) Under complex model. (b) Under simplified model.

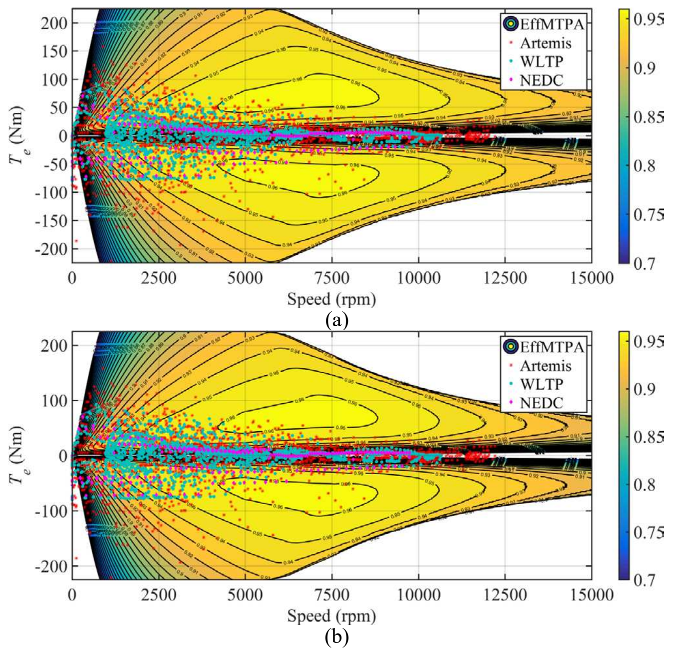

Fig. 10. Tested IPM traction machine with different driving cycles. (a) Under complex model. (b) Under simplified model.

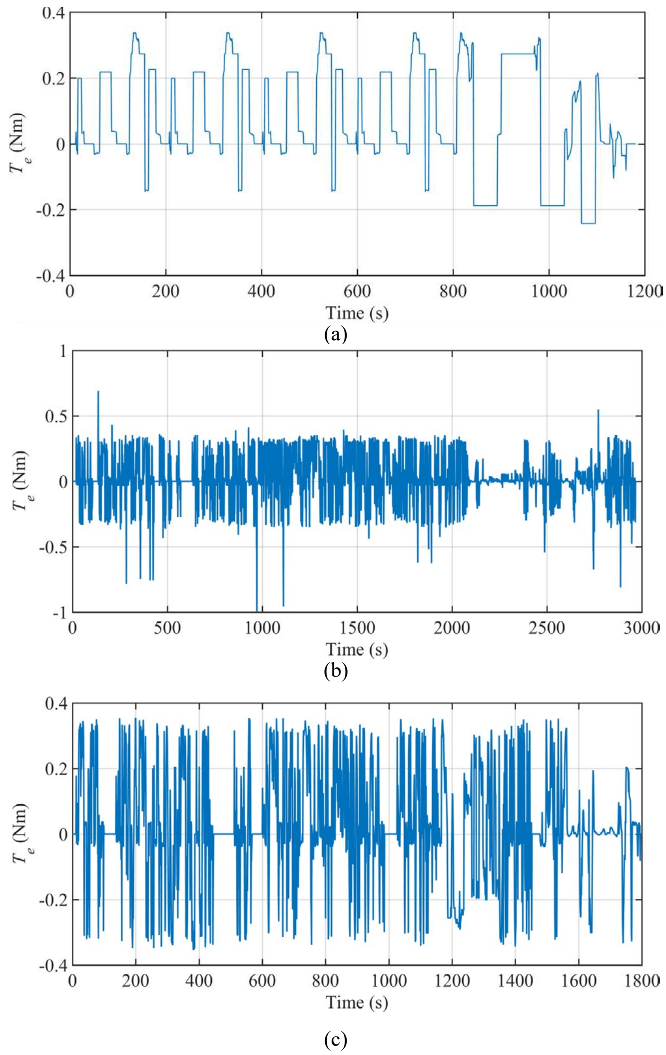

Fig. 11. Torque difference for the tested IPM traction machine under different driving cycles by employing simplified current reference LUTs. (a) NEDC. (b) Artemis. (c) WLTP.

TABLE II

ENERGY LOSSES (MJ) UNDER DIFFERENT LUTS

Driving Cycle	Complex LUT	Simplified LUT	Diff. (%)
NEDC	0.4268	0.4275	0.1640
Artemis	2.5015	2.5055	0.1596
WLTP	0.9846	0.9859	0.1319

can be seen, *dq*-axis current references generated from the simple-based model are very similar with that generated from the complex-based model with the exception of the high overload region where extreme saturation effects occur, Fig. 7.

The simplified-based current reference LUTs in Fig. 6 is employed for the tested IPM machine in Fig. 2 and the different torque in comparison with using the complex-based current reference LUTs is presented in Fig. 8. As can be seen, in the MTPA region, maximum torque error is less than 3%. On the other hand, in the FW operation region, maximum different torque is up to 12% in the boundary torque region which leads to reduction of the maximum achievable torque boundary, Fig. 8(c). It is noted that for traction application, traction machine performance is not often required for the boundary torque region. Efficiency map of the tested IPM machine for complex current reference LUTs and simplified current reference LUTs are illustrated in Fig. 9. Simplified and complex LUTs result in similar efficiency maps.

The tested IPM machine is developed for integration into a hybrid-powertrain and its performances under simplified-based and complex-based LUTs over different driving cycle is depicted in Fig. 10 and the relevant differences in torque response over different driving cycles is illustrated in Fig. 11. Again, the simplified and complex LUTs exhibit less than 1% difference in energy loss over the selected drive cycles, as shown in Table II.

Torque measurements from the tested machine at 2000rpm (MTPA operation region) under different torque

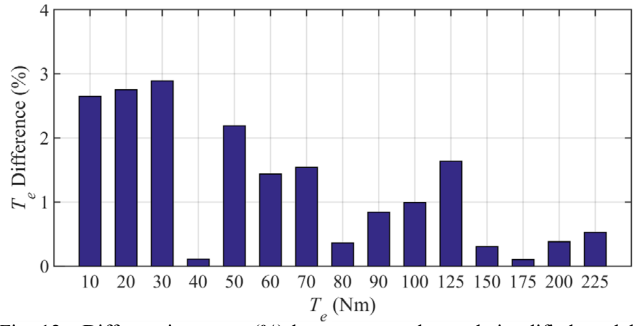

Fig. 12. Different in torque (%) between complex and simplified model at 2000rpm (MTPA operation).

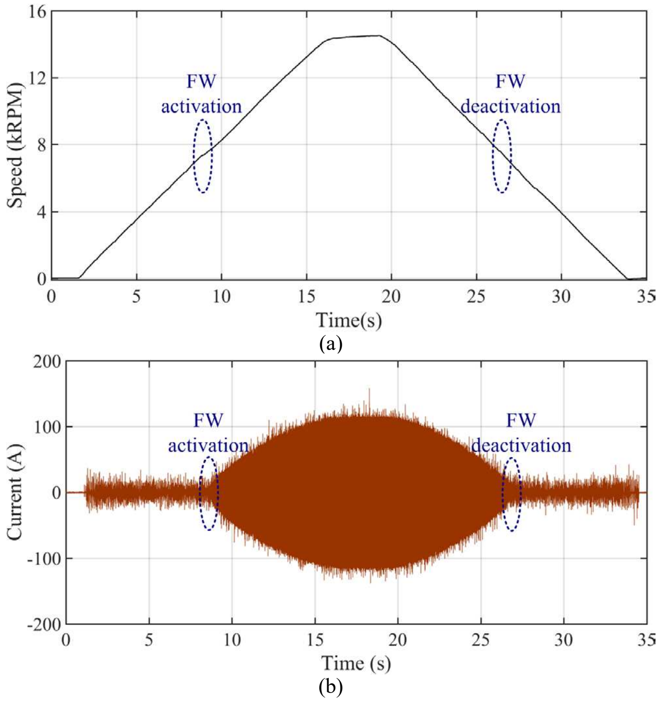

Fig. 13. Acceleration demonstration for tested IPM machine with simplified current reference LUTs. (a) Speed response. (b) Current response.

demands using both complex and simplified models are presented in Fig. 12. As can be seen, a lower than 3% difference in torque production can be achieved using the simplified model in the MTPA operation region. It is noted that this measured result is well-matched with the analysis result in Fig. 8. In addition, FW operation demonstration for the simplified model is shown in Fig. 13 where a speed acceleration for the tested IPM machine up to 14500rpm is introduced. Under no-load acceleration, the FW operation is activated for the tested IPM machine when its speed is around 7500rpm, Fig. 13. In the FW operation under no-load condition, d-axis current up to -110A-peak is required to maintain a constant voltage magnitude, Figs. 7 and 13. It is noted that in the FW operation with feed-back (FB) control technique [4], the mismatch between the current reference LUTs and the actual required currents will be compensated via the FB loop adjustment.

V. CONCLUSIONS

The paper presents a comparative evaluation of simplified and complex model for control development of IPM traction machine with single layer rotor geometry. Although implementation of the complex model could ensure better machine performances, in practice, its validation is complicated and measurement errors and temperature may compromise the control outcomes. It is shown that the simplified model which determination is significantly simpler may provide comparatively reliable control outcomes. Thus, the proposed simplified model can be considered at the earlier stages of control development of traction application. The proposed simplified model was validated via measurements in both MTPA and FW operation regions.

REFERENCES

[1] K. D. Hoang and K. Atallah, “A rapid concept development technique for electric vehicle power trains,” *in Proc. IEEE Int. Conf. Connected Vehicles and Export (ICCVE) 2014*, Vienna, Austria, Nov. 3-7, 2014, pp. 191-198.

[2] M. Kamiya, “Development of traction drive motors for the Toyota hybrid systems,” *IEEJ Trans. Ind. Appl.*, vol. 126, no. 4, pp. 473–479, Apr. 2006.

[3] K. D. Hoang, J. Wang, M. Cyriacks, A. Melkonyan and K. Kriegel, "Feed-forward torque control of interior permanent magnet brushless AC drive for traction applications," *in Proc. IEEE Int. Conf. Electric Mach. Drives (IEMDC) 2013*, Chicago, IL, US, pp. 152-159, 2013.

[4] K. D. Hoang and H. Aorith, “Online control of IPMSM drives for traction applications considering machine parameter and inverter nonlinearities,” *IEEE Trans. Transportation Electrification*, vol. 1, no. 4, pp. 312-325, Dec. 2015.

[5] B. Cheng and T. R. Tesch, “Torque feedforward control technique for permanent-magnet synchronous motors,” *IEEE Trans. Ind. Electron.*, vol. 57, no. 3, pp. 969–974, Mar. 2010.

[6] B. Stumberger, G. Stumberger, D. Dolinar, A. Hamler, and M. Trlep, “Evaluation of saturation and cross-magnetization effects in interior permanent magnet synchronous motor,” *IEEE Trans. Ind. Appl.*, vol. 39, no. 5, pp. 1264–1271, Sep./Oct. 2003.

[7] K. M. Rahman and S. Hiti, “Identification of machine parameters of a synchronous machine,” *IEEE Trans. Ind. Appl.*, vol. 41, no. 2, pp. 557– 565, Mar./Apr. 2005.

[8] R. H. Staunton, C. W. Ayers, J. N. Chiasson, B. A. Burress, and L. D. Marlino, “Evaluation of 2004 Toyota Prius hybrid electric drive system,” Oak Ridge Nat. Lab., Oak Ridge, TN, Tech. Rep. ORNL/TM- 2006/423, 2006.